Comparison of the adsorption kinetics of methylene blue using rice husk ash activated with different chemical agents

Comparação da cinética de adsorção de azul de metileno utilizando cinza de casca de arroz ativada com diferentes agentes químicos

Josiane Pinheiro Farias[1] , Carolina Faccio Demarco[1] , Thays França Afonso[1] , Leandro Sanzi Aquino[1] ,
Mery Luiza Garcia Vieira[1] , Tito Roberto Cadaval Junior[2] , Maurizio Silveira Quadro[1] , Robson Andreazza[1]

ABSTRACT

Activated carbon is widely used in several industrial sectors and has a high production cost. To reduce costs, different materials have been studied, for example, rice husks (RH). RH is an abundant, low-cost residue of the agricultural sector and can be used to generate energy due to its high calorific value. However, burning husk generates waste, the ashes. Thus, the objective of this work was to optimize the synthesis of activated carbon using pre-carbonized RH with different chemical agents as activators (KOH, NaOH, NaCl, H_2SO_4, and Na_2CO_3), at different particle sizes. Subsequently, Fourier transform infrared spectroscopy (FT-IR), scanning electron microscope (SEM), and energy dispersive spectroscopy (EDS) were used to characterize the materials. Of these, KOH was the best activating agent. The adsorption kinetics for the adsorbents was 30 min, reaching equilibrium after 70 min. Of the three fitted kinetic models, pseudo-second-order and Elovich best fit the data. The FT-IR shows that the adsorbents have oxygenated surface groups such as alcohol, ester, ether, and phenol. From the point of zero charge, the predominance of negative charges on the surface of the adsorbents is observed. Therefore, the activated carbon from rice husk ash (RHA) showed potential in the adsorption of the methylene blue dyes.

Keywords: bioenergy; application of rice husk ash; dyes.

RESUMO

O carvão ativado é amplamente utilizado em diversos setores industriais e apresenta alto custo de produção. De modo a reduzir custos, diferentes materiais vêm sendo estudados, a exemplo da casca de arroz. Esta é um resíduo abundante do setor agrícola, apresenta baixo custo de obtenção e pode ser utilizada na geração de energia graças ao seu alto poder calorífico. Contudo, a queima da casca gera resíduo, as cinzas. Assim, o objetivo do trabalho foi otimizar a síntese de carvão ativado utilizando casca de arroz pré-carbonizada com diferentes agentes químicos como ativantes (KOH, NaOH, NaCl, H_2SO_4 e Na_2CO_3), em diferentes granulometrias; e, posteriormente, espectroscopia de infravermelho por transformada de Fourier (FT-IR), microscopia eletrônica de varredura (MEV) e espectroscopia de raios X dispersiva de energia (EDS) foi aplicado na caracterização dos materiais. Destes, o KOH foi o melhor agente ativador. A cinética de adsorção para os adsorventes foi de 30 min, atingindo equilíbrio em 70 min. Dos três modelos cinéticos ajustados, pseudossegunda ordem e Elovich foram os que melhor se ajustaram aos dados. O FT-IR demonstra que os adsorventes apresentam grupos de superfícies oxigenados como álcool, éter, éster e fenol. Do ponto de carga zero em diante, observa-se a predominância de cargas negativas na superfície dos adsorventes. Sendo assim, o carvão ativado da cinza de casca de arroz mostrou-se promissor na adsorção do corante azul de metileno.

Palavras-chave: bioenergia; aplicação da cinza de casca de arroz; corante.

Introduction

Activated carbon, which is an amorphous carbonaceous material, has been recognized as a versatile material for materials science, with applications in several areas. It can be mentioned, for example, applications in industrial processes, such as the treatment of drinking water, effluents (mainly for the adsorption of metal ions, and organic molecules such as dyes), and air purification, among others. It is also used in medicine, in catalysts, and catalyst supports, such as electrode materials for batteries and supercapacitors, in natural gas and hydrogen storage processes, and in hydrogen electrosorption. The great versatility in the use of activated carbon is due to its characteristics, such as high surface area, high porosity, and the presence of functional sites on the surface (Shrestha et al., 2019; Meya et al., 2020).

Activated carbon is produced from a thermal process with low oxygen concentration or without oxygen. During carbonization, the organic substance is decomposed, and volatile parts are removed, generating material with a poorly developed porous structure, thus requiring activation.

Activation can be physical or chemical. Physical activation, also called gas activation, can use water vapor, carbon dioxide, and ozone heated to temperatures of 800–1,000°C. Chemical activation consists of mixing the precursor material or pre-carbonized coal with chemical activating agents (acids, alkalis, or salts) and heat-treating it at moderate temperatures between 400 and 800°C under an inert gas atmosphere of nitrogen or argon. The chemical agents most widely used in the activation process are $ZnCl_2$, H_3PO_4, H_2SO_4, KOH, and K_2CO_3. $ZnCl_2$ and H_3PO_4 are generally used to activate biomass of plant origin, rich in cellulose, hemicellulose, and lignin. KOH, K_2CO_3, and Na_2CO_3 are generally used to activate waste, which are rich in ash (Shrestha et al., 2019; He et al., 2020; Meya et al., 2020; Zhang et al., 2020).

Thus, several materials are successfully converted into activated carbon, such as corn cobs, citrus peel, rice peel, chitosan, peanut shells, red ceramic, coconut shells, lignin, wool, and algae, among others. However, these materials have different structures, so they produce activated carbons with different properties (Silva et al. 2017, 2018; Heidarinejad et al., 2020; Kang et al., 2020; Lestari and Chafidz, 2020; Wei et al., 2020; Zhang et al., 2020).

Among the most important properties, there is the maximum adsorption capacity (q), which can be obtained through adsorption kinetics. The adsorption kinetics can be used to evaluate the solute absorption rate, which controls the equilibrium time, as well as to predict the time required for the adsorbent and adsorbate interaction to persist. The kinetic parameters are important because they are used as a way of estimating the size and transfer rate of industrial equipment adsorption systems (Duarte Neto et al., 2018; Hubbe et al., 2019; Ahmad et al., 2020).

In most works, three kinetic models are used to describe the adsorption process, which correspond to the pseudo-first-order, pseudo-second-order, and Elovich models (De Oliveira et al., 2018; Fooladgar et al., 2019; Labaran et al., 2019; Mamaní et al., 2019; Ahmad et al., 2020). However, few works are using mathematical models in adsorption processes with the same adsorbent chemically activated with different chemical agents.

Thus, in this study, activated carbon is produced from rice husk ash (RHA) and used for the removal of methylene blue (MB) from aqueous solutions. Rice is one of the most produced and consumed cereals in the world, being one of the main foods consumed by more than half of the world's population. In Brazil, the production was 11.2 million tons of rice in the 2019/2020 crop, and an increase of 5.2% is estimated for the 2020/2021 crop (Conab, 2021), and 20% of this production, on average, is converted into waste, thus highlighting the large amount of waste generated in the form of rice husk (RH) (Nunes et al., 2017).

Due to the considerable quantities available and their low commercial value, along with their high calorific value, rice hulls are commonly used as fuel for energy generation. However, burning husk results in another residue: ash. It is estimated that for each ton of RH processed, 40 kg correspond to ash (Moraes et al., 2014; Stracke et al., 2020).

The use of RH for contaminant removal has relevance for its adsorptive potential, as well as the cost of obtaining it. Studies show that the pretreatment of RH increases the adsorption capacity, chemical treatments being more used than physical treatments (Shamsollahi and Partovinia, 2019). Thus, understanding how to improve the adsorptive process from different pre-treatments represents a great differential in the study area, aiming to increase the efficiency of MB dye removal from aqueous solutions.

Specifically, MB is a typical thiazine dye with the chemical formula $C_{16}H_{18}N_3ClS$ and is a commonly used dye in the industry (Huang et al., 2019). However, this chemical cannot be readily eliminated through conventional water treatment technologies (Kishor et al., 2021).

In this study, an optimized activated carbon production process was investigated. The raw material, pre-carbonized RH, was used for powdered activated carbon production, as an alternative, low-cost material. This work aims to verify the effect of the activation of RH ash with different chemical agents on the adsorption of MB dye, as well as to investigate the adsorption mechanism, and for such, the experimental data were modeled using the pseudo-first-order, pseudo-second-order, and Elovich models.

Materials and Methods

Activated carbon preparation

The process used to prepare the activated carbon is shown schematically in Figure 1. The RH and RHA used in this work were provided by a rice processing industry, located in Pelotas/RS. The work used only the RHA to produce activated carbon. This material was dried at 105°C for 1 hour, then sieved and segregated into two granulometry ranges: 1 mm and 0.6 mm. The sieving process was performed according to the NBR 12075/91 (ABNT, 1991).
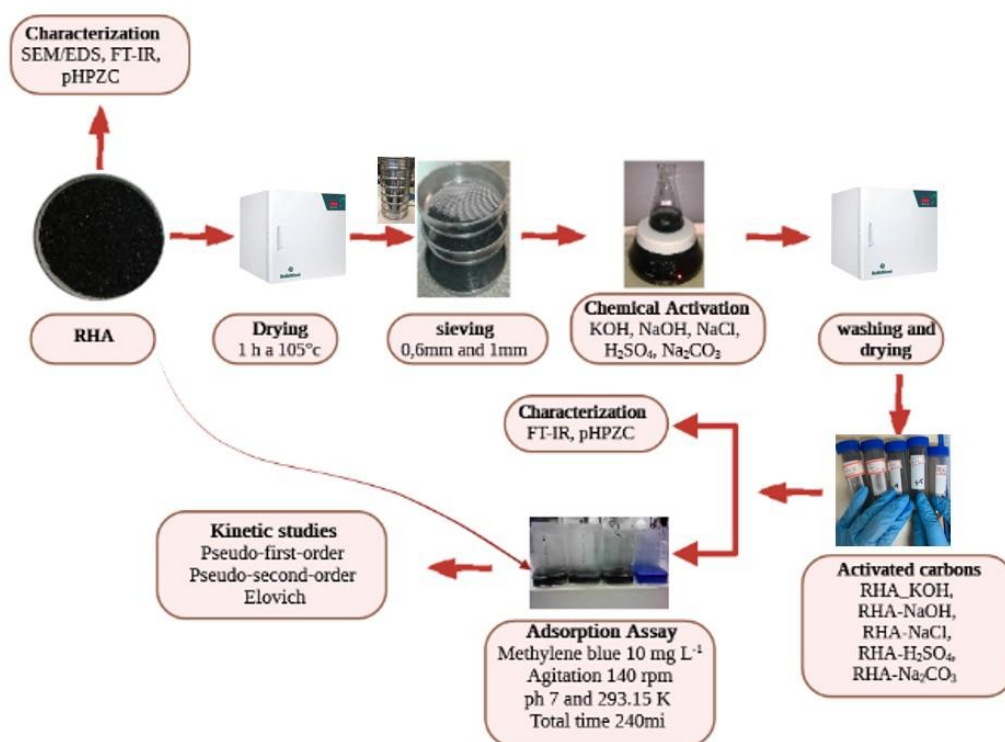
Figure 1 – Flowchart of the activated carbon production process.

In the second step, the RHA was treated separately with solutions of sodium hydroxide, potassium hydroxide, sodium chloride, sulfuric acid, and sodium carbonate, described as follows (An et al., 2011; Alvarez et al., 2014; Muniandy et al., 2014; Kaykioğlu and Güneş, 2016; Mashhadi et al., 2016):

- NaOH treatment: six grams (6 g) of ash were mixed with 50 mL of 1.5 mol L^{-1} NaOH solution. The mixture remained in dynamic contact for 24 hours.
- Treatment with KOH and NaCl: The precursors were activated by water impregnation, maintaining the mass at a 1:1 ratio of ash and activating agent, in dynamic contact for 24 hours.
- Acid Treatment (H_2SO_4): The mass of 6 g of ash was immersed in 50 ml of concentrated sulfuric acid or PA for 1 hour at a temperature of 200°C.
- Treatment with sodium carbonate (Na_2CO_3): A 6-gram portion of ash was impregnated with a 1.5 mol L^{-1} Na_2CO_3 solution for 3 hours under constant stirring.

After the treatments described above, the materials were filtered and washed several times until neutrality. Then, they were dried for 24 hours at 110°C and after drying, the samples were stored in desiccators for further use.

Characterization of RH and RHA

The elemental composition and surface morphological characteristics of RH and untreated RHA were characterized with the SEM/EDS system. The analyses were performed using a scanning electron microscope (JEOL JSM 6610, Japan). A voltage acceleration of 15 kV and magnification ranging from 50 to 2500 times were used.

The major functional groups present on the surface of the adsorbents were obtained by FT-IR spectroscopy using Shimadzu model IRPrestige-21. Spectra were recorded from 400 to 4,000 cm^{-1}, 32 scans, transmittance mode, and 4 cm^{-1} resolution.

The point of zero charge (pHPZC) was determined using 0.05 g of the charcoal in contact with 500 mL distilled water adjusted to pH values of 3 to 8 using a 0.1 mol solution of H_2SO_4 and NaOH. After 24 hours under 100 rpm stirring at room temperature, the final pH was measured (Gatabi et al., 2016). The pHPZC value for each adsorbent was obtained by the arithmetic mean of the final pH points that were constant (Giacomni et al., 2017).

Adsorption assay

The study was conducted to investigate the performance of ash treated with different chemical agents. The untreated coal and the

treated samples were placed in contact in 500 mL of an MB dye solution with an initial concentration of 10 mg L^{-1}, in a mechanical agitation process (Jar Test, New Ethic), at 140 rpm, pH 7.0, and a temperature of 293.15 K with the adsorbent dosage of 400 mg L^{-1}. The working solution was prepared with MB (97% purity, Dinâmica) and the chemical formula $C_{16}H_{18}C_1N_3S.3H_2O$.

Each assay had a total duration of 240 min, and aliquots of 3 mL of the supernatant were withdrawn at intervals of 10, 20, 30, 40, 50, 60, 70, 130, 180, and 240 min. The adsorbent was separated from the solution by centrifugation, filtration, and discontinuation of agitation. To collect these aliquots, 2 min before the pre-defined interval, the stirring was stopped to separate the phases. After collection, agitation was restarted, and this procedure was repeated for all samplings. The data were obtained in triplicate.

The concentration of the MB solution was determined by visible light spectrophotometry (Model Nova 1600 UV) at a wavelength of 665 nm. The adsorption capacity was calculated by Equation 1:

$$qt = \frac{(C_0 - C_t)v}{m} \tag{1}$$

Where:
C_0 = the initial solute concentration (mg.L^{-1});
C_t = the solute concentration at a time t (mg.L^{-1});
V = the volume of the MB solution (L);
m = the mass of adsorbent (g).

Kinetic studies

Pseudo-first-order (Ho and McKay, 1998; Cheng et al., 2017), pseudo-second-order (Ho and McKay, 1999; Lima et al., 2019), and Elovich (Low, 1960; Chien and Clayton, 1980; Bankole et al., 2019) kinetic models were used to fit the experimental data, as shown in Equations 2, 3 and 4, respectively:

$$q_t = q_1(1 - \exp(-k_1 t)) \tag{2}$$

$$q_t = \frac{t}{(1/k_2 q_2^2) + (t/q_2)} \tag{3}$$

$$q_t = 1/a \ln(1 + abt) \tag{4}$$

Where:
k1 and k2 = the pseudo-first order and pseudo-second order kinetic coefficients, respectively in (min^{-1}) and (g mg^{-1} min^{-1});
q1 and q2 = the theoretical values of adsorption capacity (mg.g^{-1});
a = the initial sorption rate due to (dq/dt) = a with qt = 0 (mg g^{-1}min^{-1});
b = the Elovich model desorption constant (g mg^{-1});
t = time (min).

The kinetic curves for each model were estimated by non-linear regression as a quasi-Newton function. The fitting of the kinetic models to the experimental data was evaluated employing the coefficients of determination (R^2) and the mean relative error (MRE).

Statistical Analysis

The ash adsorption capacity data with and without treatment at different granulometry were performed in an entirely randomized design and the results were treated by Analysis of variance (ANOVA) and, when significant, the Tukey test was performed for comparison of the means at a 5% probability level. The adjustments to the kinetic models, Tukey's test, were analyzed with the help of Statistic 7.0 software (Statsoft, USA) and the graphs constructed by the Sigma Plot software (Systat, GERMANY).

Results and Discussion

Characterization of the husk and ashes

Table 1 shows the elemental composition of both materials: RH and RHA.

The chemical composition of RH, and consequently the ash, varies depending on soil characteristics, type and content of fertilizers used, climatic conditions, and the type of rice (Nascimento et al., 2015).

Regarding the elemental composition (Table 1), it was found that the elements at higher percentages in the RH and RHA were oxygen and silica. As verified in the studies of Vieira et al. (2012) and Da Silva et al. (2016), the presence of silica in these materials influences the ability of adsorption of compounds, especially metals, because of the formation of surface charges (Tarley and Arruda, 2004; Kieling, 2009).

SEM micrographs are shown in Figure 2. From the SEM images, it can be highlighted that the structure of the outer surface of the RH (Figure 2A), which is uneven and highly rough, as well as the RHA (Figure 2B), maintains on the outside a highly rough surface and development of a porous structure.

Similar results were found in the studies of An et al. (2011) and Zhang et al. (2014), highlighting that this structure is a relevant factor to turn the RH and/or RHA into an efficient adsorbent material, demonstrating the relevance of morphological characterization for this study.

Costa and Paranhos (2019) studying the adsorption of a dye from RH and RHA also verified the existence of a well-organized external structure on the RH, with an elongated and contorted shape, similar to a corn cob, in agreement with the SEM analysis shown in this study.

The appearance of porosity on the surface of the RHA is due to the removal of lignin and cellulose present in the husk during the burning process since cellulose is the major organic constituent of the husk (Della et al., 2001).

The FT-IR spectra, as shown in Figure 3, show the presence of surface functional groups of the charcoals *in nature* and treated with different activating agents, which do not show significant differences. The highest intensity peaks 1045.66 and 1052.67 cm^{-1} can be attributed to the C - O

stretching vibration in acids, alcohols, phenols, ethers, and esters (Tongpoothorn et al., 2011; Muniandy et al., 2014; De Oliveira et al., 2018).

The band value of 614.48 cm^{-1} corresponds to in-plane ring deformation (Tongpoothorn et al., 2011). The peaks at 789.76 and 782.05 cm^{-1} are associated with the formation of the Si-O-Si bond, which is characteristic of silicate minerals (Ahmad et al., 2020; Jyoti et al., 2021).

The band at 1739.03 cm^{-1} can be attributed to the C = O carbonyl group and can be indicative of the formation of muconic acid and ester derivatives (Hoareau et al., 2004; Gatabi et al., 2016). In the spectrum, the formation of the peak at 1,359.74 and 1,352.03 cm^{-1} indicates the elongation of the aromatic C-H functional group (Srivastava et al., 2007; Shrestha et al., 2019).

Table 1 – Elemental composition of RH and RHA.

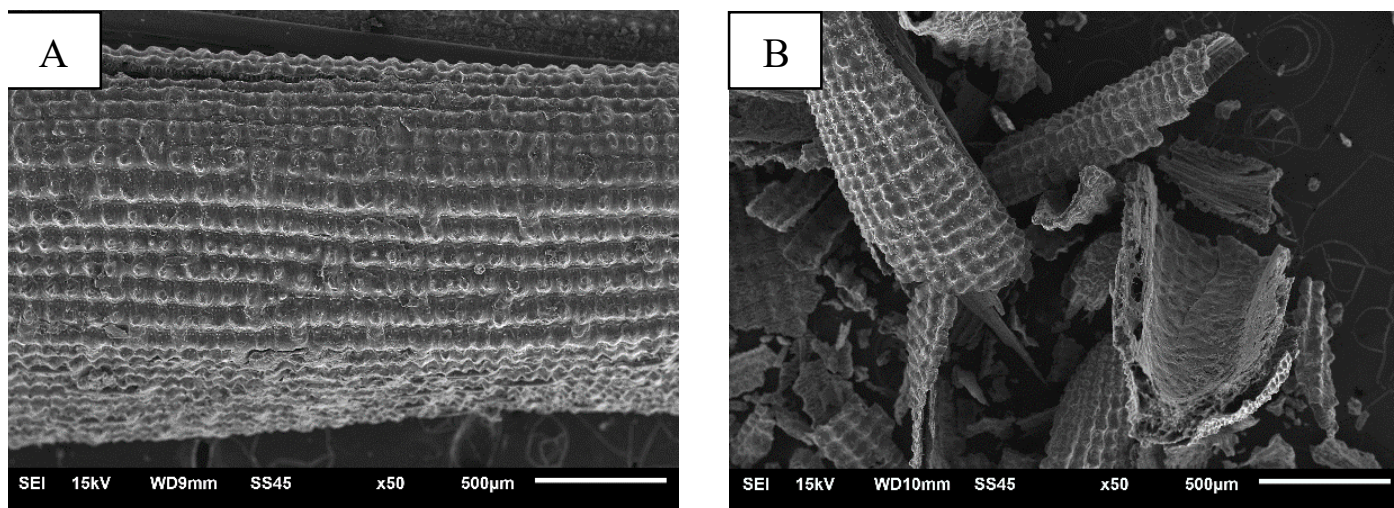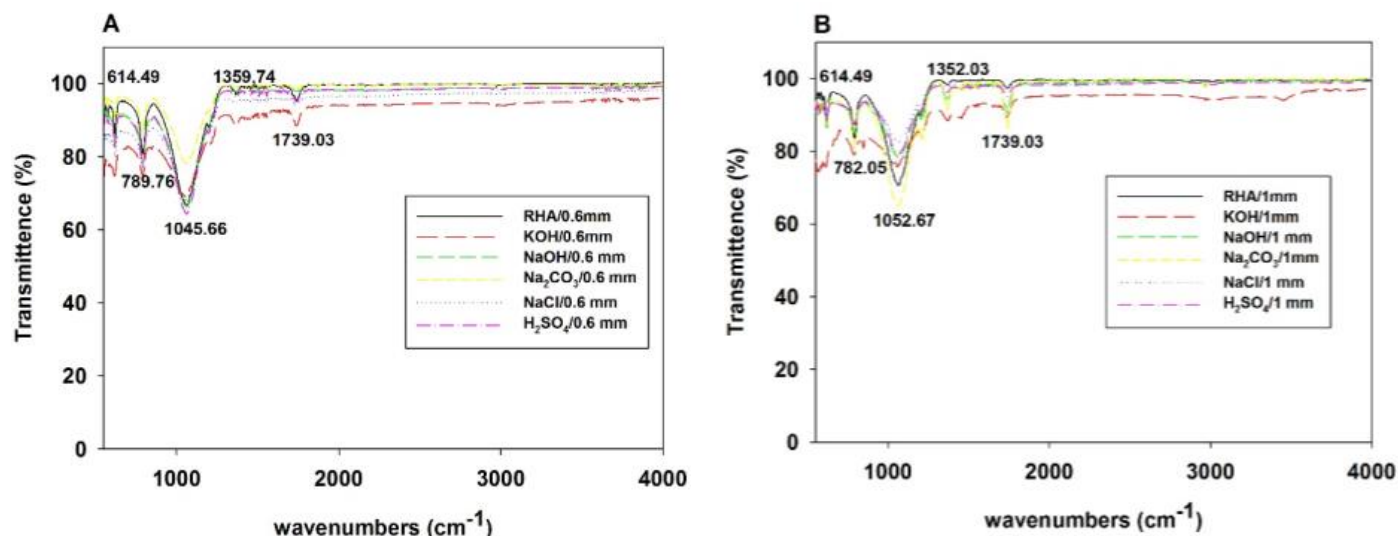| MATERIAL	ELEMENTS (%)								
	Si	C	O	Na	Al	P	S	Cl	K
RH	35.94	14.7	46.36	-	-	-	-	-	-
RHA	41.41	7.02	49.78	0.21	0.19	0.36	0.12	0.11	0.79

Figure 2 – SEM analysis; (A) RH and (B) RHA.

Figure 3 – Infrared spectra of the raw and treated ash; (A) grain size 0.6 mm and (B) grain size 1 mm.

Thus, it can be stated that the surface of the ash used in this study has oxygenated groups formed by esters, ethers, alcohols, and phenols as the main ones. These functional groups influence the reactivity and properties of the material. Adsorption of organic compounds is controlled by chemical and physical interactions, acid-base characteristics of the surface, and the presence of micropores and macropores (Belhachemi, 2021; Hummadi et al., 2022). This results in a good performance in the adsorption process of the adsorbents produced, particularly ash treated with KOH.

It is important to determine the pHPZC of the adsorbent to evaluate the ideal pH for the adsorption of dyes. Table 2 shows the values of the pHPZC of the adsorbents, produced from RHA.

As observed, the results in Table 2 for the adsorbents RHA, NaOH, KOH, H_2SO_4, NaCl, and Na_2CO_3, which have a negative surface charge, pHPZC, range from 4.98 to 6.46, being lower values than the pH 7 of the working solution (Zyoud et al., 2020).

The surface of the adsorbents has higher amounts of negative charges by the loss of protons (deprotonation of different functional groups on the surface of the biosorbent) and therefore favors the uptake of cationic dyes, such as MB, due to the increased electrostatic force of attraction (Hassan et al., 2017).

Kinetic study and statistical treatment

The contact time kinetics curves of the MB dye for the solid phase, using as adsorbent material the untreated and treated RHA, can be seen in Figure 4. In addition, for each curve, the kinetic model that best fitted the experimental data is shown, according to the coefficient of determination (R^2) and mean relative error (MRE) shown in Table 3.

The adsorption kinetics of the MB dye shows that the activated carbons produced reach equilibrium after 70 minutes, except for Na_2CO_3, which reaches equilibrium after 30 minutes. In the same way, the particle size does not change the kinetic behavior of the adsorption process of MB dye (Figures 4A and 4B).

Contact time is an important factor in an adsorption process. Usually, most of the adsorption occurs during the first 30 minutes and then increases very slowly (Khodaie et al., 2013). This behavior can be associated with the high surface area of activated carbons, which can provide massive active sites for MB adsorption. Initially, when adsorption sites are available, and the solute concentration gradient is high, the rate of adsorption of MB molecules is high. Then, the adsorption rate decreases, and a tendency to saturation is observed (Senthilkumaar et al., 2005; Mamaní et al., 2019). Several studies have reported adsorption kinetics with a time equal to or less than 60 minutes using different adsorbents in the adsorption of dyes and metal ions (Subha and Namasivayam, 2009; Mashhadi et al., 2016; Frantz et al., 2017).
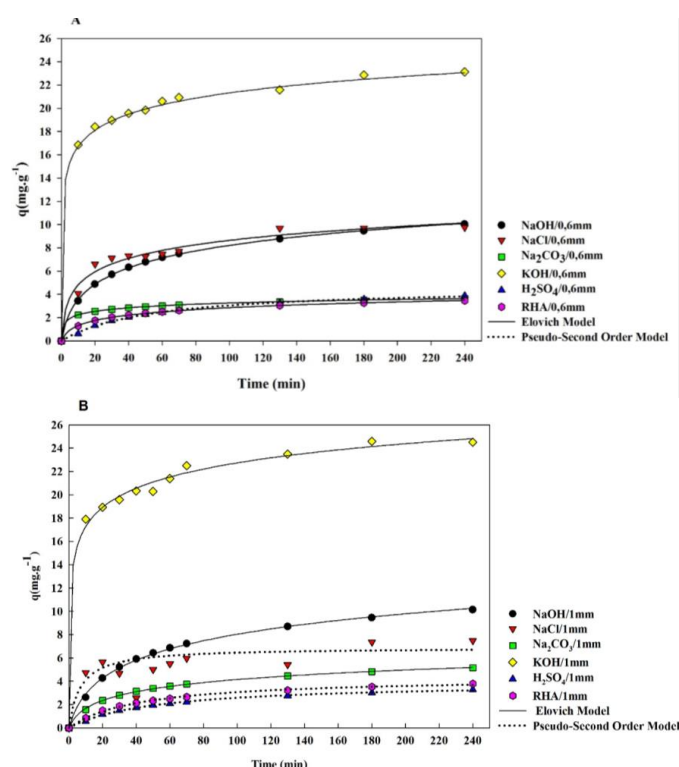

Figure 4 – (A) Contact time curves of MB adsorption for ash with and without treatment (particle size 0.6 mm), pH 7.0, temperature of 293.15 K, 140 rpm, and adsorbent dosage 400 mg L⁻¹; **(B)** Contact time curves of MB adsorption for treated and untreated ash (1 mm particle size), pH 7.0, temperature of 293.15 K, 140 rpm, and adsorbent dosage 400 mg L⁻¹.

Fast kinetics are desirable in wastewater treatment as they offer high adsorption capacity in short periods.

In this study, the treatments that obtained better performances were potassium hydroxide, sodium hydroxide, and sodium chloride. Thus, it can be stated that alkaline agents promote greater removal of silica from coal, especially when treated with potassium hydroxide because the potassium element promotes greater extraction reactivity (Muniandy et al., 2014). Another factor associated with the use of KOH is the formation of KCO_3 as an intermediate product, which implies a double activation step for this activation pathway and, consequently, greater pore development (Mamaní et al., 2019).

For NaOH, the form of silica removal is by the formation of sodium silicate, from the reaction of silica present in RHA with NaOH at room temperature, since Na_2SiO_3 is soluble in water. After washing, the material ends up leaching the silica (Schettino Jr. et al., 2007).

Table 2 – pHPZC - RHA in natura and treated.

Granulometry	RHA	NaOH	NaCl	Na_2CO_3	KOH	H_2SO_4
0.6	5.24	5.65	5.25	5.34	6.46	6.09
1	4.98	5.95	5.07	6.37	6.15	5.11

Table 3 – Calculated parameters of the evaluated kinetic models.

Granulometry (mm)	0.6 mm						1 mm					
Treatment	RHA	NaOH	NaCl	Na$_2$CO$_3$	KOH	H$_2$SO$_4$	RHA	NaOH	NaCl	Na$_2$CO$_3$	KOH	H$_2$SO$_4$
Pseudo-first order												
q$_1$ (mg.g^{-1})	3.16	9.26	8.95	3.21	20.93	3.74	3.59	9.52	6.27	4.77	22.08	3.15
k$_1$ (min^{-1})	0.03	0.03	0.05	0.09	0.14	0.02	0.02	0.02	0.14	0.03	0.14	0.02
R^2	0.953	0.960	0.924	0.932	0.958	0.991	0.984	0.978	0.871	0.968	0.935	0.99
EMR (%)	8.13	7.91	9.07	7.37	5.12	4.03	5.76	6.58	13.50	7.46	6.92	3.97
Pseudo-second order												
q$_2$ (mg.g^{-1})	3.62	10.70	10.12	3.53	22.37	4.66	4.35	11.35	6.89	5.59	23.84	3.90
k$_2$ (g.mg^{-1}min^{-1})	2.05	46.55	71.12	5.82	2711.46	1.92	1.96	39.90	48.43	5.75	2890.17	1.17
R^2	0.989	0.991	0.970	0.982	0.987	0.998	0.998	0.996	0.915	0.994	0.976	0.998
EMR (%)	3.80	3.60	5.03	3.61	2.78	3.16	1.81	2.57	10.34	3.30	4.12	2.78
Elovich												
a (g mg^{-1}min^{-1})	1.40	0.45	0.56	2.27	0.50	0.82	0.95	0.38	1.12	0.83	0.42	0.99
b (mg g^{-1})	0.38	0.89	2.69	7.09	873.42	0.12	0.16	0.537	7.12	0.36	347.58	0.11
R^2	0.999	0.999	0.975	1	0.999	0.995	0.997	0.998	0.759	0.999	0.996	0.995
EMR (%)	0.54	0.76	5.45	0.01	0.87	5.02	2.61	1.81	17.25	1.1	1.56	4.50
Experimental Capacity												
q$_{exp}$ (mg g^{-1})	3.46	10.05	9.75	3.64	23.11	3.88	3.79	10.14	7.48	5.14	24.5	3.27

The increase in adsorption efficiency with these treatments can be associated with the development of porosity formed due to the removal of silica (Schettino Jr. et al., 2007). Similar behavior was obtained by Shrestha et al. (2019) who uses RHA in the adsorption of MB treated with zinc chloride, oxidation with nitrogen gas, sodium, and potassium hydroxide, also obtained as the best treatment for potassium and sodium hydroxide, obtaining the adsorption capacity values of 608 and 80 mg g^{-1}, respectively.

Ma et al. (2019), when comparatively analyzing the contact time with higher concentrations of MB (300, 400, 500, and 600 mg L^{-1}) in a study on adsorption using activated charcoal from plant biomass - sycamore sawdust - found that equilibrium was reached after 15 minutes for the lowest concentrations of MB (300 and 400 mg L^{-1}). However, as the concentration increased, the time required to reach equilibrium also increased.

From the analysis of the kinetic study, it is highlighted that the good performance of MB adsorption demonstrated by RHA has great potential for water purification and wastewater treatment in the removal of soluble organic compounds (Shrestha et al., 2019).

Regarding particle size, the adsorption capacity values for the treatments studied did not show a significant difference, except for NaCl. This fact may be related to the very similar particle diameters. In the study of Khodaie et al. (2013), the authors found that there is an increase in the adsorption capacity of MB at the smaller the particle size, but shows approximately 153 mg g^{-1} of adsorption capacity with a particle diameter of 270 µm, and 154 mg g^{-1} with a particle diameter of 250 µm. Thus, this demonstrates that the greater the range between the diameters, the more assertive will be the study on the effect of particle size variation.

As mentioned earlier, in Table 3, the coefficient of determination (R^2 > 0.97) and the mean relative error (MRE(RME < 5.0%) are used to define the best kinetic model fit to the experimental data. Thus, according to Table 3, the pseudo-second order model was found to be the best fit to represent the kinetic data of MB dye adsorption for NaCl-treated ash (R^2 = 0.915 and EMR= 10.34), H$_2$SO$_4$ (R^2 = 0.998 and EMR= 2.78) and RHA (R^2 = 0.998 and EMR= 1.81) with 1 mm particle size and H$_2$SO$_4$ with 0.6 mm particle size (R^2 = 0.998 and EMR= 3.16). For the other treatments, the model that best fits the adsorption kinetics of the MB dye is Elovich.

As the ash treated with NaCl, H$_2$SO$_4$ and RHA with a particle size of 1 mm and H$_2$SO$_4$ with a particle size of 0.6 mm were best fit to the pseudo-second order model. Then, it can be considered that the adsorption of MB from these activations involves the mechanism of inter-in diffusion and considers that adsorption occurs through the chemical process (Piccin et al., 2012; Mashhadi et al., 2016). Therefore, the capacity values predicted at equilibrium by the model are close to the values obtained experimentally.

Mashhadi et al. (2016), in a study verifying the use of activated carbon with H$_2$SO$_4$ utilizing RH as precursor material, also verified the kinetics

of MB dye removal fitting the pseudo-second order model. The authors verified that the use of the material as an adsorbent can be recommended as a promising alternative for the removal of MB from aqueous solutions.

Similar results were found in a study conducted by Andrade-Siqueira et al. (2020) investigating the adsorption of the MB dye in another agroindustrial residue, the sugarcane bagasse. In the study, the authors also verified a fit to the pseudo-second order model, indicating the presence of a chemical process.

Another investigation about the adsorption of MB on other agro-industrial waste, soursop and sugarcane bagasse, also identified the fit of the pseudo-second order kinetic model to the experimental data (Meili et al., 2019). The authors concluded that, from the identified removal capacity and fit to the theoretical models, both types of waste represent an alternative use as an adsorbent of MB in an aqueous solution due to the low cost to obtain it and high removal performance.

For the treatments RHA/0.60 mm, NaCl/0.6 mm, and NaOH, Na_2CO_3, KOH in both granulometries, the kinetic model that best fitted the experimental data was Elovich, indicating that the adsorption process occurs by chemical interactions. This model assumes that solid surfaces are energetically heterogeneous and the kinetics is not affected by the desorption process nor by interactions between the adsorbed species, especially when it occurs under conditions of low surface coverage (Da Silva et al., 2018).

Ma et al. (2019), in a study on adsorption of MB dye on activated charcoal from plant biomass, sycamore sawdust, found that at higher concentrations (600 mg L^{-1}) the fit to the kinetic model occurred through Elovich. Other studies of MB adsorption from agroindustrial waste also verified the fit to the Elovich model (Ghaedi et al., 2014; Pezoti Jr. et al., 2014).

So, it can be stated that the adsorption of MB by the activated carbons used in the study was controlled by the process of internal diffusion and chemisorption since the pseudo-second order model and Elovich, mainly, are the models that best represent the experimental data according to Table 3.

Figure 5 shows the significant interactions between the different treatments and granulometry. The treatments that performed better in the adsorption capacity of MB dye were potassium hydroxide, sodium hydroxide, and sodium chloride. The results of adsorption capacity (Figures 4A and 4B) indicate that the treatments with sulfuric acid and sodium carbonate did not improve the adsorption performance of RHA.

The particle size variable did not show a significant difference in the performance of the adsorption capacity of the adsorbent produced from RHA, except for the treatment with sodium chloride, which shows a significant difference in the particle size variable.
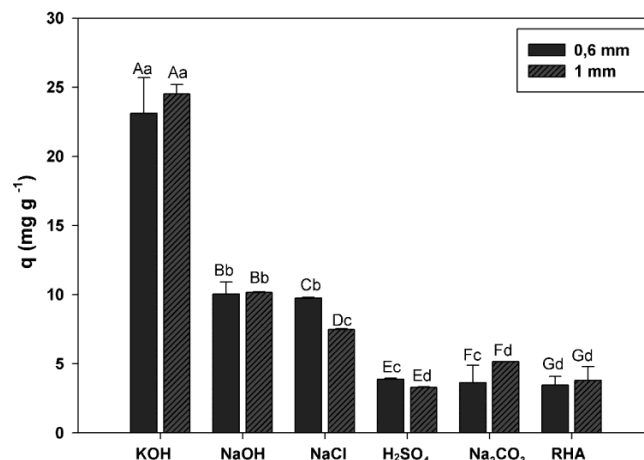

Figure 5 – MB adsorption results for ash without and with chemical treatment for particle sizes of 0.6 and 1 mm. Lowercase letters represent a significant difference by Tukey's test at 5% between treatments. Uppercase letters represent a significant difference between particle sizes.

Conclusions

The results pointed out great potential for the production of RHA activated carbon using different chemical agents. The adsorption capacity values of MB dye indicate that potassium hydroxide is the best activating agent for RHA.

The pHPZC showed that the RHA adsorbents have a predominance of negative charges on their surface. Characterization with FT-IR indicated the presence of oxygenated functional groups, alcohol, ester ether, and phenols.

The short time until equilibrium was reached demonstrates that the saturation of the surface layer of the adsorbents occurred under the kinetic conditions studied. The pseudo-second order and Elovich models are the best models that represent the experimental data. The kinetics for the material produced with RHA has internal diffusion and chemisorption as mechanisms.

The pre-carbonized RH, industrial waste, can be transformed into a product with greater added value, high-yield activated carbon, but using fewer energy resources since this study did not use the heat treatment process for carbonization and activation of coal. The reduction of primary energy consumption for industrial processes is of great environmental importance and favors the principles of sustainability. In addition, it reduces the occupation of useful areas that would be used for the construction of landfills for the disposal of this residue.

Contribution of authors:

FARIAS, J. P.: Conceptualization; Data curation; Formal Analysis; Writing – Original Draft; Writing — Review & Editing; DEMARCO, C. F.: Data curation; Writing — Original Draft; AFONSO, T. F.: Data curation; Writing — Original Draft; Writing — Review & Editing; AQUINO, L. S.: Data curation. VIEIRA, M. L. G.: Writing — Original Draft; CADAVAL JUNIOR, T. R.: Formal Analysis; Writing — Original Draft; QUADRO, M. S.: Conceptualization; Resources; ANDREAZZA, R.: Conceptualization; Resources; Writing — Original Draft; Writing — Review & Editing.

References

Ahmad, A.; Khan, N.; Giri, B. S.; Chowdhary, P.; Chaturvedi, P., 2020. Removal of methylene blue dye using rice husk, cow dung and sludge biochar: characterization, application, and kinetic Studies. Bioresource Technology, v. 306, 123202. https://doi.org/10.1016/j.biortech.2020.123202.

Alvarez, J.; Lopez, G.; Amutio, M.; Bibao, J.; Olazar, M., 2014. Upgrading the rice husk char obtained by flash pyrolysis for the production of amorphous silica and high quality activated carbon. Bioresource Technology, v. 170, 132-137. https://doi.org/10.1016/j.biortech.2014.07.073.

An, D.; Guo, Y.; Zou, B.; Zhu, Y.; Wang, Z., 2011. A study on the consecutive preparation of silica powders and active carbon from rice husk ash. Biomass And Bioenergy, v. 35, (3), 1227-1234. https://doi.org/10.1016/j.biombioe.2010.12.014.

Andrade-Siqueira, C.T.; Zanette da Silva, I.; Rubio, J.A.; Bergamasco, R.; Gasparotto, F.; Aparecida, de Souza Paccola, E.; Ueda Yamaguchi, N., 2020. Sugarcane bagasse as an efficient biosorbent for methylene blue removal: kinetics, isotherms and thermodynamics. International Journal of Environmental Research and Public Health, v. 17, (2), 526. https://doi.org/10.3390%2Fijerph17020526.

Associação Brasileira de Normas Técnicas (ABNT), 1991. Carvão ativado pulverizado - Especificação - EB-2133. ABNT, Rio de Janeiro.

Bankole, M.T.; Abdulkareem, A.S.; Mohammed, I.A.; Ochigbo, S.S.; Tijani, J.O.; Abubakre, O.K.; Roos, W.D., 2019. Selected heavy metals removal from electroplating wastewater by purified and polyhydroxylbutyrate functionalized carbon nanotubes adsorbents. Scientific Reports, v. 9, 4475. https://doi.org/10.1038/s41598-018-37899-4.

Belhachemi, M., 2021. Chapter 14 - Adsorption of organic compounds on activated carbons. Sorbents Materials for Controlling Environmental Pollution, Current State and Trends, 355-385. https://doi.org/10.1016/B978-0-12-820042-1.00006-7.

Cheng, S.; Zhang, L.; Xia, H.; Peng, J.; Shu, J.; Li, C.; Jiang, X.; Zhang, Q., 2017. Adsorption behavior of methylene blue onto waste-derived adsorbent and exhaust gases recycling. RSC Advances, v. 7, (44), 27331-27341. https://doi.org/10.1039/C7RA01482A.

Chien, S.H.; Clayton, W.R., 1980. Application of elovich equation to the kinetics of phosphate release and sorption in soils. Soil Science Society of America Journal, v. 44, (2), 265-268. https://doi.org/10.2136/sssaj1980.03615995004400020013x.

Companhia Nacional de Abastecimento (Conab), 2021. Acompanhamento da safra brasileira de grãos, v. 8, safra 2020/21, n. 10, Conab, Brasília (Accessed in July, 2021) at:. http://www.conab.gov.br.

Costa, J.A.S.; Paranhos, C.M., 2019. Evaluation of rice husk ash in adsorption of remazol red dye from aqueous media. SN Applied Sciences, v. 1, 397. https://doi.org/10.1007/s42452-019-0436-1.

Da Silva, J.E.; Rodrigues, F.I.L.; Pacífico, S.N.; Santiago, L.F.; Munix, C.R.; Saraiva, G.D.; Nascimento, R.F.; Viente Neto, O.S., 2018. Study of kinetics and adsorption equilibrium employing chemically modified coconut shell for the removal of Pb(Ii) from synthetic bath. Revista Virtual de Química, v. 10, (5), 1248-1262. https://doi.org/10.21577/1984-6835.20180086.

Da Silva, P.R.N.; Gonçalves, G.R.; Freitas, J.C.C., 2016. Preparation, characterization and evaluation in gasification of cellulignins derived from sugar cane bagasse and rice husks: reuse case of lignocellulosic waste. Revista Virtual de Química, v. 8, (5), 1262-1276. https://doi.org/10.21577/1984-6835.20160091.

De Oliveira, F.M.; Coelho, L.M.; De Melo, E.I., 2018. Evaluation of the adsorption process using green coconut mesocarp for removal of methylene blue dye. Revista Matéria, v. 23, (4), e12223. https://doi.org/10.1590/s1517-707620180004.0557.

Della, V.P.; Kühn, I.; Hotza, D., 2001. Caracterização de cinza de casca de arroz para uso como matéria-prima na fabricação de refratários de sílica. Química Nova, v. 24, (6), 778-782. https://doi.org/10.1590/S0100-40422001000600013.

Duarte Neto, J.F.; Pereira, I.D.S.; Da Silva, V.C.; Ferreira, H.C.; Neves, G.A.; Menezes, R.R., 2018. Study of equilibrium and kinetic adsorption of rhodamine b onto purified bentonite clays. Cerâmica, v. 64, (372), 598-607. https://doi.org/10.1590/0366-69132018643722429.

Fooladgar, S.; Teimouri, A.; Nasab, S.G., 2019. Highly efficient removal of lead ions from aqueous solutions using chitosan/rice husk ash/nano alumina with a focus on optimization by response surface methodology: isotherm, kinetic, and thermodynamic studies. Journal of Polymers and the Environment, v. 27, (5), 1025-1042. https://doi.org/10.1007/s10924-019-01385-3.

Frantz, T.S.; Silveira Jr., N.; Quadro, M.S.; Andreazza, R.; Barcelos, A.A.; Cadaval Jr., T.R.S.; Pinto, L.A.A., 2017. Cu(ii) adsorption from copper mine water by chitosan films and the matrix effects. Environmental Science and Pollution Research, v. 24, (6), 5908-5917. https://doi.org/10.1007/s11356-016-8344-z.

Gatabi, M.P.; Moghaddam, H.M.; Ghorbani, M., 2016. Point of zero charge of maghemite decorated multiwalled carbon nanotubes fabricated by chemical precipitation method. Journal of Molecular Liquids, v. 216, 117-125. https://doi.org/10.1016/j.molliq.2015.12.087.

Ghaedi, M.; Nasab, A.G.; Khodadoust, S.; Rajabi, M.; Azizian, S., 2014. Application of activated carbon as adsorbents for efficient removal of methylene blue: kinetics and equilibrium study. Journal of Industrial and Engineering Chemistry, v. 20, (4), 2317-2324. https://doi.org/10.1016/j.jiec.2013.10.007.

Giacomni, F.; Menegazzo, M.A.B.; Da Silva, M.G.; Da Silva, A.B.; De Barros, M.A.S.D., 2017. Point of zero charge of protein fibers, an important characteristic for dyeing. Revista Materia, v. 22, (2), e11827. https://doi.org/10.1590/S1517-707620170002.0159.

Hassan, W.; Farooq, U.; Ahmad, M.; Athar, M.; Khan, M.A., 2017. Potential biosorbent, haloxylon recurvum plant stems, for the removal of methylene blue dye. Arabian Journal of Chemistry, v. 10, (Suppl. 2), S1512-S1522. https://doi.org/10.1016/j.arabjc.2013.05.002.

He, W.Y.; Liao, W.; Yang, J.Y.; Jeyakumar, P.; Abderson, C., 2020. Removal of vanadium from aquatic environment using phosphoric acid modified rice straw. Bioremediation Journal, v. 24, (1), 80-89. https://doi.org/10.1080/10889868.2020.1724073.

Heidarinejad, Z.; Dehghani, M.H.; Heidari, M.; Javedan, G.; Ali, I.; Sillanpaa, M., 2020. Methods for preparation and activation of activated carbon: a review. Environmental Chemistry Letters, v. 18, 393-415. https://doi.org/10.1007/s10311-019-00955-0.

Ho, Y.S.; McKay, G., 1998. Sorption of dye from aqueous solution by peat. Chemical Engineering Journal, v. 70, (2), 115-124. https://doi.org/10.1016/S0923-0467(98)00076-1.

Ho, Y.S.; McKay, G., 1999. Pseudo-second order model for sorption processes. Process Biochemistry, v. 34, (5), 451-465. https://doi.org/10.1016/S0032-9592(98)00112-5.

Hoareau, W.; Trindade, W.G.; Siegmund, B.; Castellan, A.; Frollini, E., 2004. Sugar cane bagasse and curaua lignins oxidized by chlorine dioxide and reacted with furfuryl alcohol: characterization and stability. Polymer

287

Degradation and Stability, v. 86, (3), 567-576. https://doi.org/10.1016/j.polymdegradstab.2004.07.005.

Huang, Y.F.; Zhu, J.M.; Liu, H.E.; Wang, Z.Y.; Zhang, X.X., 2019. Preparation of porous graphene/carbon nanotube composite and adsorption mechanism of methylene blue. SN Appled Sciences, v. 1, (1), 37. https://doi.org/10.1007/s42452-018-0035-6.

Hubbe, M.; Azizian, S.; Douven, S., 2019. Implications of apparent pseudo-second-order adsorption kinetics onto cellulosic materials: a review. Bioresources, v. 14, (3), 7582-7626.

Hummadi, K.K.; Luo, S.; He, S., 2022. Adsorption of methylene blue dye from the aqueous solution via bio-adsorption in the inverse fluidized-bed adsorption column using the torrefied rice husk. Chemosphere, v. 287, (Part 1), 131907. https://doi.org/10.1016/j.chemosphere.2021.131907.

Jyoti, A.; Singh, R.K.; Kumara, N.; Amana, A.K.; Kar, M., 2021. Synthesis and properties of amorphous nanosilica from rice husk and its composites. Materials Science and Engineering, v. 263, 114871. https://doi.org/10.1016/j.mseb.2020.114871.

Kang, S.; Quin, L.; Zhao, Y.; Wang, W.; Zhang, T.; Yang, L.; Rao, F.; Song, S., 2020. Enhanced removal of methyl orange on exfoliated montmorillonite/chitosan gel in presence of methylene blue. Chemosphere, v. 238, 124693. https://doi.org/10.1016/j.chemosphere.2019.124693.

Kaykioğlu, G.; Güneş, E., 2016. Kinetic and equilibrium study of methylene blue adsorption using H_2SO_4– activated rice husk ash. Desalination And Water Treatment, v. 57, (15), 7085-7097. https://doi.org/10.1080/19443994.2015.1014859.

Khodaie, M.; Ghasemi, N.; Moradi, B.; Rahimi, M., 2013. Removal of methylene blue from wastewater by adsorption onto $ZnCl_2$ activated corn husk carbon equilibrium studies. Journal of Chemistry, v. 2013, 383985. https://doi.org/10.1155/2013/383985.

Kieling, A.G., 2009. Influência da segregação no desempenho de cinzas de casca de arroz como pozolanas e material adsorvente. Doctora thesis, Unisinos, São Leopoldo.

Kishor, R.; Saratale, G.D.; Saratale, R.G.; Ferreira, L.F.R.; Bilal, M.; Iqbal, H.M.N.; Bharagava, R.N., 2021. Efficient degradation and detoxification of methylene blue dye by a newly isolated ligninolytic enzyme producing bacterium *Bacillus albus* MW407057. Colloids and Surfaces B: Biointerfaces, v. 206, 111947. https://doi.org/10.1016/j.colsurfb.2021.111947.

Labaran, A.N.; Zango, Z.U.; Armaya, U.; Garba, Z.N., 2019. Rice husk as biosorbent for the adsorption of methylene blue. Science World Journal, v. 14, (2), 66-70.

Lestari, A.Y.D.; Chafidz, A., 2020. Production of activated carbon from agro-industrial wastes and its potential use for removal of heavy metal in textile industrial wastewater. In: Zakaria, Z.; Aguilar, C.; Kusumaningtyas, R.; Binod, P. (Eds.), Valorisation of agro-industrial residues. Applied environmental science and engineering for a sustainable future. Springer, Cham, pp. 127-144, v. 2. https://doi.org/10.1007/978-3-030-39208-6_6.

Lima, H.H.C.; Maniezzo, R.S.; Llop, M.E.G.; Kupfer, V.L.; Arroyo, P.A.; Guolherme, M.R.; Rubira, A.F.; Girotto, E.M.; Rinaldi, A.W., 2019. Synthesis and characterization of pecan nutshell-based adsorbent with high specific area and high methylene blue adsorption capacity.Journal of Molecular Liquids, v. 276, 570-576. https://doi.org/10.1016/j.molliq.2018.12.010.

Low, M.J.D., 1960. Kinetics of chemisorption of gases on solids. Chemical Reviews, v. 60, (3), 267-312. https://doi.org/10.1021/cr60205a003.

Ma, P.; Wang, S.; Wang, T.; Wu, J.; Xing, X.; Zhang, X., 2019. Effect of bifunctional acid on the porosity improvement of biomass-derived activated carbon for methylene blue adsorption. Environmental Science and Pollution Research, v. 26, (29), 30119-30129. https://doi.org/10.1007/s11356-019-06177-9.

Mamaní, A.; Ramírez, N.; Deiana, C.; Giménez, M.; Sardella, F., 2019. Highly micro porous sorbents from lignocellulosic biomass: different activation routes and their application to dyes adsorption. Journal of Environmental Chemical Engineering, v. 7, (5), 103148. https://doi.org/10.1016/j.jece.2019.103148.

Mashhadi, S.; Javadian, H.; Ghasemi, M.; Saleh, T.A.; Gupta, V.K., 2016. Microwave-induced H2so4 activation of activated carbon derived from rice agricultural wastes for sorption of methylene blue from aqueous solution. Desalination And Water Treatment, v. 57, (44), 21091-21104. https://doi.org/10.1080/19443994.2015.1119737.

Meili, L.; Lins, P.V.S.; Costa, M.T.; Almeida, R.L.; Abud, A.K.S.; Soletti, J.I.; Dotto, G.L.; Tanabe, E.H.; Sellaoui, L.; Carvalho, S.H.V.; Erto, A., 2019. Adsorption of methylene blue on agroindustrial wastes: experimental investigation and phenomenological modelling. Progress in Biophysics and Molecular Biology, v. 141, 60-71. https://doi.org/10.1016/j.pbiomolbio.2018.07.011.

Meya, E.; Olupot, P.W.; Storz, H.; Lubwama, M.; Kiros, Y.; John, M.J., 2020. Optimization of pyrolysis conditions for char production from rice husks and its characterization as a precursor for production of activated carbon. Biomass Conversion and Biorefinery, v. 10, (53), 57-72. https://doi.org/10.1007/s13399-019-00399-0.

Moraes, C.A.; Fernandes, I.J.; Calheiro, D.; Kieling, A.G.; Brehm, F.A.; Rigon, M.R.; Berwanger Filho, J.A.; Schneider, I.A.; Osório, E., 2014. Review of the rice production cycle: by-products and the main applications focusing on rice husk combustion and ash recycling. Waste Management and Research, v. 32, (11), 1034-1048. https://doi.org/10.1177/0734242X14557379.

Muniandy, L.; Adam, F.; Mohamed, A.R.; Ng, E.P., 2014. The synthesis and characterization of high purity mixed microporous/mesoporous activated carbon from rice husk using chemical activation with NaOH and KOH. Microporous and Mesoporous Materials, v. 197, 316-323. https://doi.org/10.1016/j.micromeso.2014.06.020.

Nascimento, G.C.; Dominguini, L.; Mello, J.M.M.; Magro, J.D.; Riella, H.G.; Fiori, M.A., 2015. Caracterização físico-química da cinza de casca de arroz oriunda do processo termelétrico do Sul de Santa Catarina – Brasil. Ciência e Natura, v. 37, (3), 634-640. https://doi.org/10.5902/2179460X15262.

Nunes, O.M.; Borges, G.R.; Wohlemberg, J.; Rodrigues, E.D.; Mathias, L.R.; Lopes, L., 2017. Rice hull as alternative energy: A case study in the municipality of dom Pedrito – RS. Igepec Toledo, v. 21, (2), 42-62.

Pezoti Jr., O.; Cazetta, A.L.; Souza, I.P.A.F.; Bedin, K.C.; Martins, A.C.; Silva, T.L.; Almeida, V.C., 2014. Adsorption studies of methylene blue onto zncl2-activated carbon produced from buriti shells (Mauritia Flexuosa L). Journal of Industrial and Engineering Chemistry, v. 20, (6), 4401-4407. https://doi.org/10.1016/j.jiec.2014.02.007.

Piccin, J.S.; Gomes, C.S.; Feris, L.A.; Gutterres, M., 2012. Kinetics and isotherms of leather dye adsorption by tannery solid waste. Chemical Engineering Journal, v. 183, 30-38. https://doi.org/10.1016/j.cej.2011.12.013.

Schettino Jr., M.A.; Freitas, J.; Cunha, A.; Emmerich, F.; Soares, A.; Silva, P.R., 2007. Preparação e caracterização de carvão ativado quimicamente a partir da casca de arroz. Química Nova, v. 30, (7), 1663-1668. https://doi.org/10.1590/S0100-40422007000700031.

Senthilkumaar, S.; Varadarajan, P.R.; Porkodi, K.; Subbhuraam, C.V., 2005. Adsorption of methylene blue onto jute fiber carbon: kinetics and equilibrium studies. Journal of Colloid and Interface Science, v. 284, (1), 78-82. https://doi.org/10.1016/j.jcis.2004.09.027.

Shamsollahi, Z.; Partovinia, A., 2019. Recent advances on pollutants removal by rice husk as a bio-based adsorbent: a critical review. Journal of Environmental Management, v. 246, 314-323. https://doi.org/10.1016/j.jenvman.2019.05.145.

Shrestha, L.M.; Thapa, R.; Shrestha, R.G.; Maji, S.; Pradhananga, R.R.; Ariga, K., 2019. Rice husk-derived high surface area nanoporous carbon materials with excellent iodine and methylene blue adsorption properties. Journal of Carbon Research, v. 5, (1), 10. https://doi.org/10.3390/c5010010.

Silva, A.B.C.; Andrade, R.M.F.; Freire, F.B.; Nagalli, A.; Carvalho, K.; Passig, F.H.; Kreutz, C., 2017. Análise da utilização de cerâmica vermelha como adsorvente na remoção do corante têxtil direct blue de uma solução aquosa. Revista. Matéria, v. 22, (3), 1-14. https://doi.org/10.1590/s1517-707620170003.0202.

Silva, T.; Barbosa, C.; Gama, B.; Nascimento, G.; Duarte, M.M.M.B., 2018. Agregação de valor a resíduo agroindustrial: remoção de fenol utilizando adsorvente preparado a partir de casca de amendoim. Revista Matéria, v. 23, (1), e11947. https://doi.org/10.1590/s1517-707620170001.0283.

Srivastava, V.C.; Mall, I.D.; Mishra, I., 2007. Adsorption thermodynamics and isosteric heat of adsorption of toxic metal ions onto bagasse fly ash (BFA) and rice husk ash (RHA). Chemical Engineering Journal, v. 132, (1-3), 267-278. https://doi.org/10.1016/j.cej.2007.01.007.

Stracke, M.P.; Girardello, V.C.; Zwirtes, E.; Nagel, J.C.; Tusset, B.T.K., 2020. Rice bark gray as a molecular water reservoir for soy production. Brazilian Journal of Development, v. 6, (1), 949-962. https://doi.org/10.34117/bjdv6n1-066.

Subha, R.; Namasivayam, C., 2009. Zinc chloride activated coir pith carbon as low-cost adsorbent for removal of 2,4-dichlorophenol: equilibrium and kinetic studies. Indian Journal of Chemical Technology, v. 16, (6), 471-479.

Tarley, C.R.T.; Arruda, M.A.Z., 2004. Biosorption of heavy metals using rice milling by-products. Characterisation and application for removal of metals from aqueous effluents. Chemosphere, v. 54, (7), 987-995. https://doi.org/10.1016/j.chemosphere.2003.09.001.

Tongpoothorn, W.; Sriuttha, M.; Homchan, P.; Chanthai, S.; Ruangviriyachai, C., 2011. Preparation of activated carbon derived from Jatropha curcas fruit shell by simple thermo-chemical activation and characterization of their physico-chemical properties. Chemical Engineering Research and Design, v. 89, (3), 335-340. https://doi.org/10.1016/j.cherd.2010.06.012.

Vieira, M.G.A.; De Almeida Neto, A.F.; Da Silva, M.G.C.; Nóbrega, C.C.; Melo Filho, A.A., 2012. Characterization and use of in natura and calcined rice husks for biosorption of heavy metals ions from aqueous effluents. Brazilian Journal of Chemical Engineering, v. 29, (3), 619-633. https://doi.org/10.1590/S0104-66322012000300019.

Wei, H.; Wang, H.; Heqing, L.; Cui, D.; Dong, M.; Lin, J.; Fran, J.; Zhang, J.; Hou, H.; Shi, Y.; Zhou, D.; Guo, Z., 2020. Advanced porous hierarchical activated carbon derived from agricultural wastes toward high performance supercapacitors. Journal of Alloys And Compounds, v. 820, 153111. https://doi.org/10.1016/j.jallcom.2019.153111.

Zhang, S.; Zhu, S.; Zhang, H.; Liu, X.; Xiong, Y., 2020. Synthesis and characterization of rice husk-based magnetic porous carbon by pyrolysis of pretreated rice husk with $FeCl_3$ And $ZnCl_2$. Journal of Analytical and Applied Pyrolysis, v. 147, 104806. https://doi.org/10.1016/j.jaap.2020.104806.

Zhang, Y.; Zheng, R.; Zhao, J.; Ma, F.; Zhang, Y.; Meng, Q., 2014. Characterization Of H_3PO_4-treated rice husk adsorbent and adsorption of copper (Ii) from aqueous solution. Biomed Research International, v. 2014, 496878. https://doi.org/10.1155%2F2014%2F496878.

Zyoud, A.H.; Asaad, S.; Samer, H.; Zyoud, S.H.; Zyoud, S.H.; Helal, M.A.; Qamhieh, N.; Hajamohideen, A.; Hilal, H.S., 2020. Raw clay supported ZnO nanoparticles in photodegradation of 2-chlorophenol under direct solar radiations. Journal of Environmental Chemical Engineering, v. 8, (5), 104227. https://doi.org/10.1016/j.jece.2020.104227.